A new compact model coupling rainfall-runoff and routing model to support reservoir releases management

S. Munier, J. Lerat, G. Belaud, X. Litrico

A new compact model coupling rainfall-runoff and routing model to support reservoir releases management

Simon Munier[(1)], Julien Lerat[(2)], Gilles Belaud[(3)], Xavier Litrico[(1)]

[(1)] Cemagref Montpellier, UMR G-EAU, 361 rue J.F. Breton, BP 5095, 34196 Montpellier Cedex 5, France, email: simon.munier@cemagref.fr, xavier.litrico@cemagref.fr
[(2)] Cemagref Antony, Parc de Tourvoie, BP 44, 92163 Antony Cedex, France, email: julien.lerat@cemagref.fr
[(3)] IRD, UMR G-EAU, Maison des Sciences de l'Eau, 300 Avenue Emile Jeanbrau, 34095 Montpellier Cedex 5, France, email: belaud@msem.univ-montp2.fr

Abstract

The article proposes a model for integrated management of a regulated watershed. In such systems, it is important to take into account not only the discharge released at the reservoir, but also the natural flows due to rainfall. The proposed model incorporates both inputs, and can be refined by considering different numbers of sub-basins corresponding to tributaries of the river. We discuss the parameter identification and show that the validation is improved when the discharge transfer inputs are used in the model. These upstream discharge inputs correspond to reservoir releases in the case of a regulated watershed. The model is tested on data from the Tarn river in South-Western France.

1 Introduction

In many regulated watersheds, the reservoirs are used to release water in order to simultaneously satisfy withdrawals along a river reach and guarantee flow at certain critical points. When these points are distant from the reservoir, the managers must account for the transfer time as well as the possible contributions of the catchment area. For the design of real time regulation tools, it is necessary to elaborate compact models for the flow routing so as to predict the behavior of the river during various events (dam release for example). However this transfer can be influenced by lateral inflows, in particular the contributions due to the rainfall, which are generally underestimated in the existing routing methods.

The purpose of this paper is to establish a compact model of flow routing integrating the contributions due to the rainfalls. This model results from the coupling of a flow routing model and a rainfall-runoff model. The flow routing model is a physical model, based on the linearized Saint-Venant equations transposed in the Laplace domain. The downstream discharge is then expressed analytically with respect to the upstream discharge (dam release), and to lateral inflows distributed along the river reach. The lateral inflows result from a rainfall-runoff model applied to the catchment area, which is divided into sub-basins

whose runoff ends in a point of the principal river. The flow resulting from the rainfall-runoff model is then distributed between the sub-basins according to their respective surfaces, and is introduced into the river in the form of lateral inflow located at each sub-basin mouth. In that way, the flow routing model takes the catchment contributions into account. The integrated model is applied to a catchment area presenting a dam at the upstream end, a set point (reserved flow) at the downstream and intermediate tributaries.

2 Problem statement and methodology

We consider the watershed of a river stretch where the upstream discharge $Q_u(t)$, function of time t, may be controlled thanks to releases from a reservoir dam. At the downstream end of the river stretch, the discharge $Q_d(t)$ is measured and must always be superior to a critical threshold Q_{min}, also called reserved discharge, thanks to dam releases. Water withdrawals for irrigation or domestic use may occur along the river, that dam releases must compensate for in order to ensure the reserved discharge. Therefore, it is essential to accurately evaluate the transit time in the river. For the reservoir manager, it is also essential to avoid releasing too much water. A rainfall in the watershed could lead to reduce the required release, provided its effect on the flow dynamics and amount are well considered.

The present article proposes a new method of coupling a production function (e.g., rainfall-runoff function) to the flow routing process in a stream. The considered system is composed of two types of inputs: the upstream discharge $Q_u(t)$ and the climate data, $P(t)$ (rainfall) and $PE(t)$ (potential evapotranspiration). The system output is the downstream discharge $Q_d(t)$. In the dam release control framework, $Q_u(t)$ can be adjusted by the dam manager according to management objectives. To this end, the manager needs transfer functions to evaluate the flow routing in the river stretch and the influence of the rainfall on the downstream discharge. In the context of real-time operation, the simulations must be quick.

Here, we analyze how the transfer functions of the two types of input interact. We first consider the flow routing model ($Q_u(t) \rightarrow Q_d(t)$). Then, we establish the transfer function of a distributed flow along the river stretch, which is referred to as the lateral inflow in the following ($q_l(x,t)$). Finally, the transfer function $P(t) - PE(t) \rightarrow q_l(x,t)$ is established using a rainfall-runoff model.

To calibrate such a model, a set of parameters has to be identified, based on the minimization of the error between simulated output ($Q_s(t)$) and measured output ($Q_m(t)$). The identifiability of such a system is generally a problem since several sets of parameters may give the same response (see e.g. Beven, 2001).

The basis of the approach is to derive the flow routing model from simple and easily accessible characteristics of the river stretch. Modeling of flow routing in a river stretch has been the subject of numerous publications since the 1950s. A comprehensive review of approximate flow routing methods has been presented by Weinmann and Laurenson (1979). Different linear models have been developed for flow routing simulation purposes (e.g. (Dooge et al., 1987a; Tsai, 2003)). Most of them are based on an analysis of the linearized Saint-Venant equations around a reference flow. The downstream boundary condition is usually neglected by considering a semi-infinite channel (see e.g., Dooge et al., 1987a) because it greatly simplifies the equations. This point may be questionable in the context of dam release management which has generally to be done in low flow. In such a context, the natural of artificial cross structures (weirs) may induce backwater

and feedback effects. Munier et al. (2007) proposed a method to take these effects into account in the transfer function. This transfer function is based on a simplification of the water surface profile and the linearization of the Saint-Venant's equations. The Laplace transform of the equations leads to the transfer function in the Laplace domain. Coupled with a cross structure discharge equation, one gets a transfer function taking account of the backwater and feedback effects due to the cross structure.
The same framework is adopted here, since the transfer function can be easily calculated based on a few characteristics of the river stretch: mean slope, mean discharge, mean river width and roughness coefficient. When available, information about the cross structures (usually weirs) can also be used.
The effect of a lateral inflow on the river dynamics has been studied by a few researchers. The methods are generally based on the linearization of a transfer model (Saint-Venant or a simplification) and the transfer function in the Laplace domain. Moussa (1996) analyzed the effect of a uniform lateral inflow on the flow dynamics established from the linearized diffusive wave equation. An extension of this study on the complete Saint-Venant's equations is proposed by Moramarco et al. (1999). More recently, Fan and Li (2006) studied the influence of localized or uniformly distributed in a finite channel. The main limitations of these approaches is the use of the convolution product to calculate the transfer in the temporal domain, which is time-consuming and represent a limitation in the context of real-time operation.
In this paper, we propose an approximation of the transfer functions of the lateral inflow in the Laplace domain, which leads to first order plus delay transfer functions. These functions lead to input delayed first-order differential equations in the time domain, which are calculated more quickly than the convolution product.
Still, there are multiple manners to consider the inflow due to rain: this inflow can be considered as uniformly distributed, distributed according to the drained area, considered as punctual (case of a well identified tributary) or a combination of these methods. This point is discussed in section 4 with an illustration on a 82km long stretch of the upper Tarn River (South of France).

3 Theoretical framework

3.1 The Linear Lag-an-Route (LLR) transfer model

The transfer model is set to provide the discharge at any point in the channel with respect to several localized lateral inflows. This section presents the methodology.

3.1.1 General methodology

We consider a semi-infinite rectangular channel with localized lateral inflows q_l (see Fig. 1).
The full one-dimensional Saint-Venant equations are linearized around a reference uniform steady state regime. These equations are then rewritten in the Laplace domain, which leads, under the considered assumptions, to one Saint-Venant transfer function per lateral discharge linking the discharge at any point in the channel to the corresponding lateral discharge. Because of the difficulty to inverse the obtained discharge back to the time domain, the moment matching method is applied in order to simplify the transfer functions. This method ensures a low frequency approximation, well adapted to the free

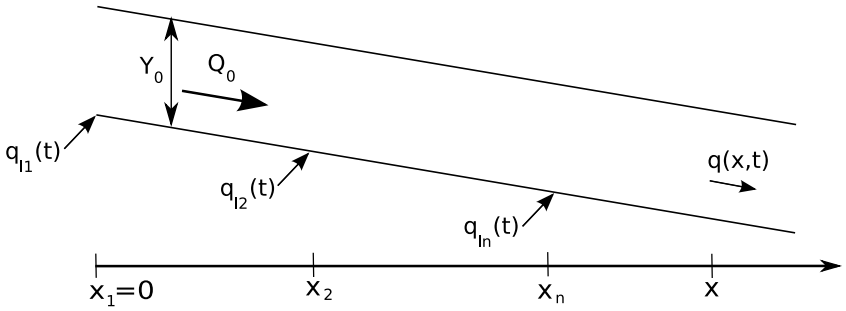

Figure 1: General scheme of the considered channel.

surface transfer, and provides simplified transfer functions TF_i of the form of a first order plus delay (attenuation plus delay), corresponding in the time domain to a simple first order ordinary differential equation.
The obtained model is referred to as LLR for *linear lag-and-route* model.

3.1.2 Linearized Saint-Venant equations

We consider a stationary regime and small variations around it. The stationary regime (reference flow) is characterized by constant discharge Q_0 and corresponding normal water depth Y_0 along the channel, and no lateral inflows.
The following notations are used: x (m) is the abscissa along the channel, B the channel width, S_b the bed slope and g the gravitational acceleration (ms^{-2}). The following variables represent the reference flow: A_0 the wetted area (m^2), P_0 the wetted perimeter (m), Q_0 the discharge (m^3/s) through section A_0, Y_0 the water depth (m), S_{f0} the friction slope, $V_0 = Q_0/A_0$ the mean flow velocity (ms^{-1}), T_0 the top width (m), $F_0 = V_0/C_0$ the Froude number with $C_0 = \sqrt{gA_0/T_0}$ the wave celerity (ms^{-1}). Throughout the article, the flow is assumed to be subcritical (i.e., $F_0 < 1$).
The friction slope S_{f0} is modeled using the Manning formula (see Chow, 1988):

$$S_{f0} = \frac{Q_0^2 n^2}{A_0^2 R_0^{4/3}} \tag{1}$$

with n the Manning coefficient ($\mathrm{sm}^{-1/3}$) and R_0 the hydraulic radius (m), defined by $R_0 = A_0/P_0$.
Let us denote $q(x,t)$, $y(x,t)$ and $q_l(x,t)$ the variations in discharge, water depth and lateral inflow at abscissa x and time t, compared to the reference steady state regime.
The linearized Saint-Venant equations are given by (see Litrico and Fromion (2004a) for details):

$$T_0 \frac{\partial y}{\partial t} + \frac{\partial q}{\partial x} = q_l \tag{2}$$

$$\frac{\partial q}{\partial t} + 2V_0 \frac{\partial q}{\partial x} - \mu_0 q + \left(C_0^2 - V_0^2\right) T_0 \frac{\partial y}{\partial x} - \nu_0 y = 0 \tag{3}$$

where the dependency on x and t is omitted for readability.
In the general non-uniform case, parameters ν_0 and μ_0, which are functions of x, are

defined by the following equations:

$$\nu_0 = V^2\frac{dT}{dx} + gT\left[(1+\kappa)S_b - (1+\kappa-(\kappa-2)F^2)\frac{dY}{dx}\right] \quad (4)$$

$$\mu_0 = -\frac{2g}{V}\left(S_b - \frac{dY}{dx}\right) \quad (5)$$

with $\kappa = 7/3 - 4A/(3TP)(\partial P/\partial Y)$.

The boundary conditions are given by the upstream discharge $q(0,t)$ and the lateral inflow denoted $q_l(x,t)$. The lateral inflow is considered as the sum of n lateral discharges $q_{li}(t)$ localized at different longitudinal positions x_{li}, $i = 1 \ldots n$ (Eq. 6). One may note that the upstream discharge can be considered as a lateral discharge localized at the upstream end of the channel ($x = 0$).

$$q_l(x,t) = \sum_{i=1}^{n} \delta(x - x_{li}) q_{li}(t) \quad (6)$$

where δ is the Dirac function.

3.1.3 Saint-Venant Transfer Function

Since the model is linear, the contribution of each lateral inflow q_{li} can be computed separately and finally added to obtain the discharge at any point in the channel.
The Saint-Venant equations are expressed in the frequency domain using the Laplace transform. A time function expressed as $f(t)$ in the time domain is expressed as $f(s)$ in the Laplace domain, where s is the Laplace variable. The transposition to the Laplace domain allowed us to solve these equations analytically, leading to a closed-form expression of Saint-Venant transfer functions $TF_i(x,s)$ corresponding to each lateral inflow. These transfer functions lead to analytical expressions of the contribution $q_i(x,s)$ of the lateral inflow $q_{li}(s)$ localized at x_i to the discharge $q(x,s)$ at any point in the channel.

$$q(x,s) = \sum_{i=1}^{n} q_i(x,s) \quad (7)$$

$$q_i(x,s) = TF_i(x,s) q_{li}(s), \qquad i = 1..n \quad (8)$$

The Saint-Venant transfer function relative to one particular localized lateral inflow is computed following the method developed in Munier et al. (2007). The Saint-Venant transfer function $TF_i(x,s)$ at the relative distance x corresponding to the lateral inflow $q_{li}(s)$ localized at x_i, is given by Eq. (9).

$$TF_i(x,s) = \frac{(\lambda_2 - 2bs)e^{-\lambda_1 x_i} - (\lambda_1 - 2bs)e^{-\lambda_2 x_i}}{\lambda_2 - \lambda_1} e^{\lambda_1 x} \quad (9)$$

where

$$\lambda_j = a + bs + (-1)^j\sqrt{(2ad + c^2)s^2 + 2acs + a^2}$$

and $a = \frac{\nu_0}{2T_0(C_0^2 - V_0^2)}$, $b = \frac{V_0}{C_0^2 - V_0^2}$, $c = \frac{V_0\nu_0 - (C_0^2 - V^2)T\mu_0}{\nu_0(C_0^2 - V_0^2)}$, $d = \frac{1}{2a}\left[\frac{C_0^2}{(C_0^2 - V_0^2)^2} - c^2\right]$.
Eq. (9) provides a linear distributed model for lateral inflow transfer in a semi-infinite open-channel. This model is expressed analytically in the frequency domain by a transcendental transfer function which depends on the pool characteristics.

One may remark that the Hayami transfer model is a particular case of the one presented here. Indeed the Hayami model is based on the diffusive wave equation, which is deduced from the complete Saint-Venant equations by neglecting the inertia terms. This last assumption leads to a simplified expression of the eigenvalues $\lambda_1 = \frac{C_e - \sqrt{C_e^2 + 4D_e s}}{2D_e}$ and $\lambda_2 = \frac{C_e + \sqrt{C_e^2 + 4D_e s}}{2D_e}$ ($C_e = -\nu_0/\mu_0 T_0$ and $D_e = -gA_0/\mu_0 T_0$) which correspond to the ones of the Hayami model. Additionally, the transfer function corresponding to an upstream inflow ($x_l = 0$) is given by $TF(x,s) = e^{\lambda_1 x}$. Consequently, the channel transfer model presented here is an extension of the Hayami model allowing us to take the complete Saint-Venant equations with localized lateral inflows into account.

3.1.4 Low frequency approximate transfer function

The method provides a simple expression of the discharge $q(x,s)$ at any point in the channel in the Laplace domain. To express it in the time domain ($q(x,t)$), one usually uses the convolution operation. Then, Eqs. (7–8) can be represented by:

$$q(x,t) \quad = \quad \sum_{i=1}^{n} TF_i(x,t) * q_{li}(t) \tag{10}$$

where $f * g$ represent the convolution of the two functions f and g, and is defined by $(f*g)(t) = \int_{-\infty}^{+\infty} f(t-\tau)g(\tau)d\tau$. The convolution can be implemented numerically, but its execution can be very time consuming.
Another possibility is to simplify the expression of the transfer function in the frequency domain. It is well-known that the flow routing in a channel is a delayed process, and that there is some attenuation of the peak flow. Such phenomenon can be accurately described by a rational transfer function with delay. To enable analytical computations, we restrict ourselves to a first order with delay model (Eq. (11)), as it is classically done in the literature (Malaterre (1994); Rey (1990)). We show in the following that using the classical moment matching method (see Dooge et al. (1987a); Rey (1990)), one may identify the parameters of a first order with delay that matches the low order moments of the full Saint-Venant transfer function given by Eq. 9.

$$\tilde{TF}_i(x,s) = \frac{G_i(x)e^{-\tau_i(x)s}}{1 + K_i(x)s} \tag{11}$$

The R-th cumulant (i.e., logarithmic moment) of a transfer function h is given by:

$$M_R[h(x,t)] = (-1)^R \frac{d^R}{ds^R}[\log h(x,s)]_{s=0} \tag{12}$$

The purpose of the moment matching method is to match the cumulants of the exact transfer function to those of the approximate one. Equating the first n cumulants of the exact transfer function and the approximate one ensures a good representation for the low frequency range.
$M_{i0}(x)$, $M_{i1}(x)$ and $M_{i2}(x)$ denote the first three cumulants of the transfer function $TF_i(x,s)$ given by Eq. (9), computed using the Taylor series expansion at $s = 0$. One may note that $M_{i0}(x) = 1$, which is in agreement with the mass conservation law.

Equating the first three cumulants of the approximate transfer function $\tilde{TF}_i(x,s)$ to $M_{i0}(x)$, $M_{i1}(x)$ and $M_{i2}(x)$ leads to:

$$\begin{cases} G_i(x) = 1 \\ K_i(x) = \sqrt{M_{i2}(x)} \\ \tau_i(x) = M_{i1}(x) - \sqrt{M_{i2}(x)} \end{cases} \tag{13}$$

One may note that other approximate models can be set with the present method, since it simply requires to solve the system obtained by equating the first cumulants of the transfer function and its approximation. In particular, adding a zero in the transfer function may lead to a better approximation for short canals (see Litrico and Fromion (2004a)).
In any case, this method leads to analytical and distributed expressions of the model parameters (τ_i, K_i, $i = 1..n$). These expressions provide a low frequency approximation of the flow transfer. Parameters are obtained analytically as functions of the physical parameters of the pool (geometry, friction, discharge). Since the approximate model $\tilde{TF}_i(x,s)$ is a first order with delay, the contribution q_i of lateral inflow q_{li} to the discharge at any point in the channel verifies the following ordinary differential equation:

$$K_i(x)\frac{d}{dt}q_i(x,t) + q_i(x,t) = q_{li}(t - \tau_i(x)) \tag{14}$$

using a numerical scheme to solve this equation (e.g. with a Runge-Kutta algorithm) is generally less time consuming than computing the convolution.

3.2 Rainfall-Runoff model

The GR4J model is a four parameters conceptual lumped rainfall-runoff model. Streamflows at the outlet of a catchment are calculated from rainfall and potential evapotranspiration (PE) time-series in seven steps: first, net rainfall P_n and potential evapotranspiration PE_n are determined with a zero capacity interception store:

$$\begin{array}{ll} P \geq PE \Rightarrow P_n = P - PE & PE_n = 0 \\ P < PE \Rightarrow P_n = 0 & PE_n = E - P \end{array} \tag{15}$$

Second, in the case where Pn is different from 0, a soil moisture accounting store (SMA) is filled by a part P_s of the net rainfall determined by the following equation:

$$P_s = \frac{X_1\left(1 - \left(\frac{S}{X_1}\right)^2\right)\tanh\left(\frac{P_n}{X_1}\right)}{1 + \frac{S}{X_1}\tanh\left(\frac{P_n}{X_1}\right)} \tag{16}$$

Where X_1 is the capacity of the SMA store and S the water level in the same store. In the case where P_n is null and $E_n > 0$, an evaporation rate E_s is computed to evaporate water from the SMA store with the following equation:

$$E_s = \frac{S\left(2 - \left(\frac{S}{X_1}\right)\right)\tanh\left(\frac{E_n}{X_1}\right)}{1 + \left(1 - \frac{S}{X_1}\right)\tanh\left(\frac{E_n}{X_1}\right)} \tag{17}$$

Third, leakages from the SMA store is finally calculated to account for slow contributions with the following equation:

$$Perc = S\left\{1 - \left[1 + \left(\frac{4}{9}\frac{S}{X_1}\right)\right]\right\} \tag{18}$$

The water level in the SMA store is finally updated with all the preceeding terms: $S = S + P_s - Es - Perc$.
Four, effective rainfall P_r is calculated as the remaining of the net rainfall after withdrawal from SMA store and addition of percolation: $P_r = P_n - Ps + Perc$. This effective rainfall is then partitioned into two components: 90% of P_r are routed by a unit hydrograph $UH1$ and a non linear routing store as a slow component, 10% of P_r are routed with a second unit hydrograph $UH2$ as a fast component. $UH1$ has a time base of X_4, $UH2$ of $2 \times X_4$. The reader is referred to Perrin et al. (2003) for the exact formulation of unit hydrographs.
Five, an intercatchment groundwater flow function is computed to account for gain or losses due to interactions with neighboring catchments or groundwater:

$$F = X_2\left(\frac{R}{X_3}\right)^{7/2} \tag{19}$$

Where R is the water level in the routing store, X_3 the routing store capacity and X_2 the intercatchment groundwater flow parameter.
Six, the routing store water level is updated with the output from the $UH1$ hydrograph Q_{UH1} and the gain or losses term F if the balance is positive: $R' = \max(0, R + Q_{UH1} - F)$.
Output Q_r from the routing reservoir is calculated by the following equation:

$$Q_r = R\left\{1 - \left[1 + \left(\frac{R}{X_3}\right)\right]^{4/3}\right\} \tag{20}$$

Seven, the final discharge at the catchment outlet is calculated as the sum of routing reservoir output Q_r and the output of $UH2$ noted Q_{UH2} minus the gain and losses term applied on the fast component if the balance is positive:

$$Q = Q_r + \max(0, Q_{UH2} + F) \tag{21}$$

Figure 2 present the overall model scheme. The interested reader is referred to Perrin et al. (2003) for additional details. Finally, the four parameters to be calibrated are the following:

1. X_1, the capacity of the soil moisture store (in millimeters),
2. X_2, the exchange parameter that controls the intercatchment groundwater flows (in millimeters). Positive values traduce water imports from groundwater or neighbouring catchments, negative values imply water exports,
3. X_3, the capacity of the routing store (in millimeters),
4. X_4, the time base of the unit hydrograph (in days). This parameter controls the time lag between effective rainfall and runoff peaks.

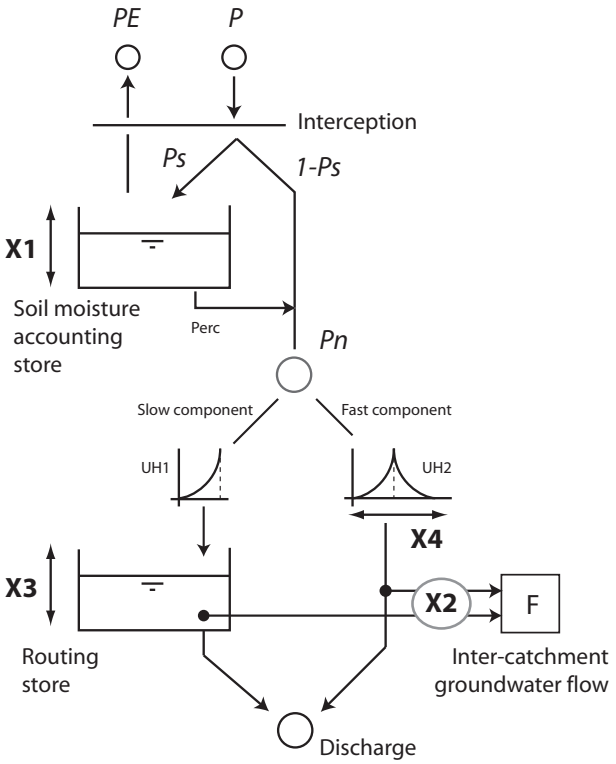

Figure 2: GR4J rainfall-runoff model scheme

3.3 Compact integrated model

At this stage, two sub-models have been computed: the first one, the lag-and-route model, provides the downstream discharge from the upstream discharge and localized lateral inflows, and the second one, the rainfall-runoff model, transforms the rainfall over a basin into a discharge at its downstream end. These two sub-models are then coupled to get the integrated model: the sub-basins of the main tributaries and the remaining sub-basin are considered, the GR4J model takes the rainfall and potential evapotranspiration over each sub-basin as inputs and computes the discharge at their downstream end; the LLR model takes the upstream discharge and the outputs of the GR4J model as inputs and computes the discharge at the downstream end of the reach. The integrated model is then determined by eight parameters: four for the lag-and-route model and four for the rainfall-runoff model.

Over-parametrization can occur when a model has too many degrees of freedom: many different sets of parameters can provide similar responses to a given input. In order to avoid this problem, we used the physical property of the lag-and-route model and reduced the calibration exercise to the identification of GR4J parameters. Since the parameters of this model are physically based, they can be estimated *a priori*. The reference discharge Q_0 is set to the mean value of the upstream discharge, the channel width B is set to the average width of the river, the bed slope S_b can be deduced from the reach length and the altitude of the upstream and downstream stations and the Manning coefficient n can be determined from the characteristics of the river bed (see reference values in Chow, 1988). Then, the four parameters X_1, X_2, X_3 and X_4 of the rainfall-runoff model GR4J are chosen to maximize the Nash-Sutcliffe coefficient NS on a first temporal period:

$$NS = 1 - \frac{\sum_{i=1}^{N} \left(Q_s(t_i) - Q_m(t_i)\right)^2}{\sum_{i=1}^{N} \left(Q_m(t_i) - \overline{Q_m}\right)^2} \tag{22}$$

where N is the number of time samples of the identification period, $Q_s(t_i)$ and $Q_m(t_i)$ the simulated downstream discharge and the measured downstream discharge respectively, at time t_i, and $\overline{Q_m}$ the mean measured values of the downstream discharge.
For validation, the obtained set of parameters is used to simulate the discharge on a second period. The quality of the prediction is evaluated by the Nash-Sutcliffe coefficient too.

4 Results and discussion on a case study

4.1 Presentation of the case study

The integrated model have been tested on the particular case of the upper Tarn basin. The area of this basin if 946 km^2. The considered reach is defined by two measurement stations. The sub-basin relative to the upstream station is not considered, its area is 10 km^2. The reach length is 82 km. The sub-basin between the upstream end and the downstream end of the reach is called intermediate basin S_0. The two main tributaries are located at 23 km and 62 km, their relative sub-basins S_1 and S_2 have an area of 263 km^2 and 119 km^2 respectively. Fig. 3 shows a representation of the upper Tarn basin.

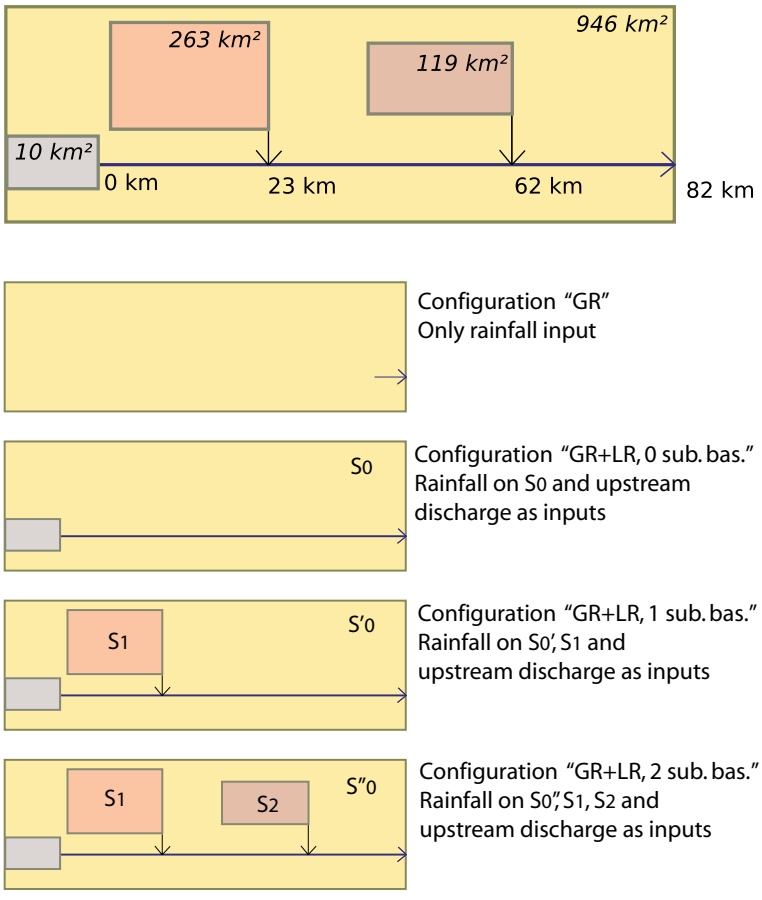

Figure 3: Representation of the upper Tarn basin.

Hourly rainfall and PE are available over the period from 01/01/96 to 31/12/04 in four different spatial configurations:

- GR: Mean areal rainfall and PE (MAR&PE) are calculated on the overall catchment.
- GR+LR, 0 sub-basin: MAR&PE are calculated on the intermediate catchment S_0 between the upstream and downstream stations.
- GR+LR, 1 sub-basin: MAR&PE are calculated on the catchment of the first tributary S_1 and on the remaining intermediate area S_0'.
- GR+LR, 2 sub-basins: MAR&PE are calculated on the catchment of the first and the second tributary S_2 and on the remaining intermediate area S_0''.

For the considered reach, the parameters of the LLR model are resumed in table 1.

Q_0	B	S_b	n
0.554 m^3/s	100 m	7.8 10^{-3} m/m	0.04

Table 1: LLR parameters for the considered reach.

In this study case, results of different models are compared. The first one is the GR4J model without accounting for the routing from the upstream end to the downstream end of the reach (classical lumped mode). The second one is the integrated model just with the intermediate basin S_0. The third one is the integrated model accounting for the sub-basin S_1, and the last one is the integrated model accounting for S_1 and S_2 (intermediate area is then reduced to S_0' and S_0'' respectively).
The identification step is done on the period from 01/01/96 to 31/12/99, whereas the validation step is done on the period from 01/01/01 to 31/12/04.

4.2 Parameter identification

The identification step is applied on the four models. Table 2 summarizes the sets of the GR parameters that maximize the Nash-Sutcliffe criterion for each model.

	GR	GR+LR: 0 sub-basin	GR+LR: 1 sub-basin	GR+LR: 2 sub-basin
X_1	306	304	380	350
X_2	−0.16	0.058	−0.0031	0.083
X_3	190	181	93.1	94.9
X_4	15.2	18.3	22.3	20.0

Table 2: Parameter identification.

These parameters are classical values for GR4J.
One will note the evolution of the parameter set when introducing additional tributaries. This traduces the strong impact of lateral inflow discretization on hydrological parameters. For each model, the Nash-Sutcliffe criterion is reported in table 3. This criterion is better when the rainfall-runoff model is applied on the whole intermediate basin S_0 and the upstream discharge is routed through the river reach using the LLR model. The criterion decreases when accounting for one or two sub-basins.

GR	GR+LR: 0 sub-basin	GR+LR: 1 sub-basin	GR+LR: 2 sub-basin
86.2%	87.8%	84.0%	83.7%

Table 3: Nash-Sutcliffe criterion for the identification step.

Fig. 4 shows the downstream discharge simulated Q_d by the GR4J model applied alone and by the integrated model without any sub-basin compared to the measured downstream discharge. This graph shows that the three discharges are very close (the Nash-Sutcliffe criterion is 86.2% for the GR model and 87.8% for the integrated model).

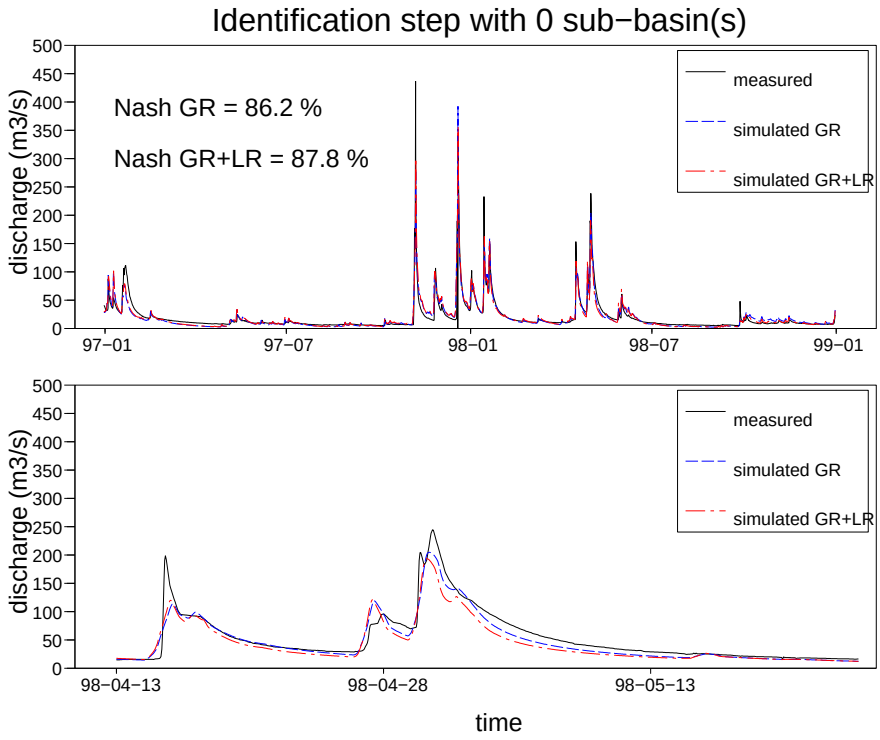

Figure 4: Identification step. Discharge at the downstream end of the channel (on the whole identification period and zoom): (− −) measurements, (· · ·) GR simulation, (—) GR+LR simulation without any sub-basin.

4.3 Validation step

The four models are then validated on a four years period, from 01/01/01 to 31/12/04. Table 4 summarizes the Nash-Sutcliffe criterion for each model on the validation period.

GR	GR+LR: 0 sub-basin	GR+LR: 1 sub-basin	GR+LR: 2 sub-basin
75.2%	77.9%	82.7%	82.2%

Table 4: Nash-Sutcliffe criterion for the validation step.

The table shows that, firstly, accounting for the routing of the upstream discharge through the river reach in the transformation of the rainfalls into the discharge at the downstream end of the basin, improves the reconstitution of the downstream discharge. Secondly,

taking the sub-basin relative to the main tributary into account also improves the reconstitution. However, taking the sub-basin relative to the second tributary does not increase the Nash-Sutcliffe criterion.
Fig. 5 shows the downstream discharge simulated by the GR model and by the integrated model without any sub-basin, compared to the measured downstream discharge. Fig. 6 shows the same graph, but the integrated model takes one sub-basin into account.

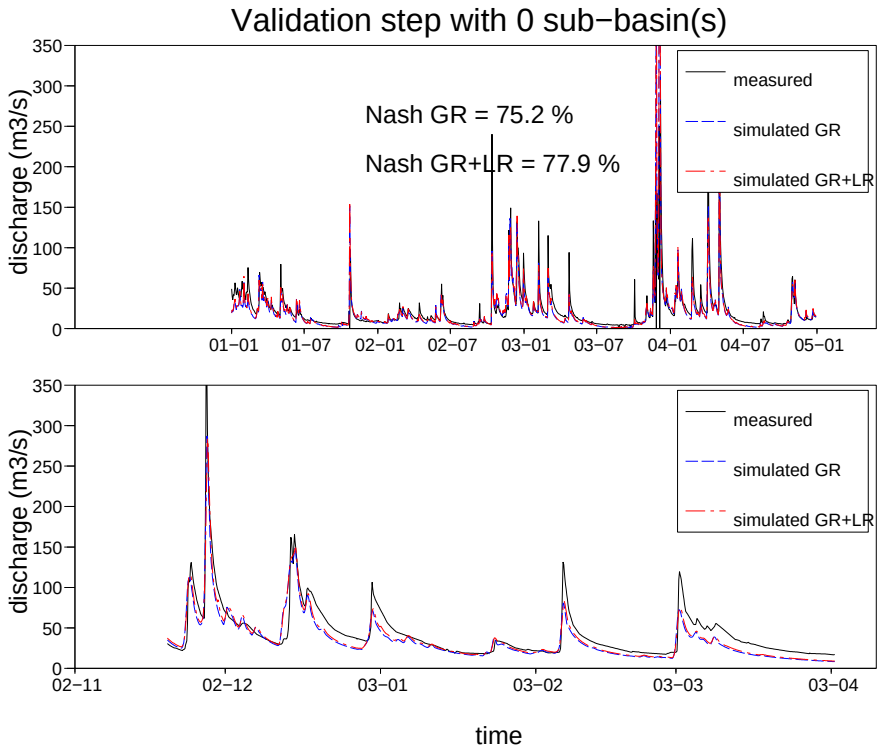

Figure 5: Validation step. Discharge at the downstream end of the channel (on the whole validation period and zoom): (− −) measurements, (· · ·) GR simulation, (——) GR+LR simulation without any sub-basin.

4.4 Discussion

In the identification process, the performance of the model is quite similar between the different configurations: the quality of the prediction is almost unsensitive to the model structure. However, the validation step clearly shows an improvement when considering the upstream discharge in the downstream discharge prediction, even though the upstream basin is very small compared to the whole basin. This means that the upstream discharge brings an important contribution to the predicted discharge. When considering one sub-basin, the Nash-Sutcliffe coefficient improves by 7.5% compared to the lumped model. Adding more sub-basins does not necessarily improve the prediction, as we can see from table 4. There may be many reasons why the performance is not improved with more sub-basins, such as uncertainties in data and model, but the results suggest that the key factors are not in the flow routing process.
It is clear too that the method of identification favors the reconstitution of the rainy events, and the low flows seem to be rather poorly simulated (Fig. 5 and 6). Different error coefficients may be used, according to the relative importance of the low flows and

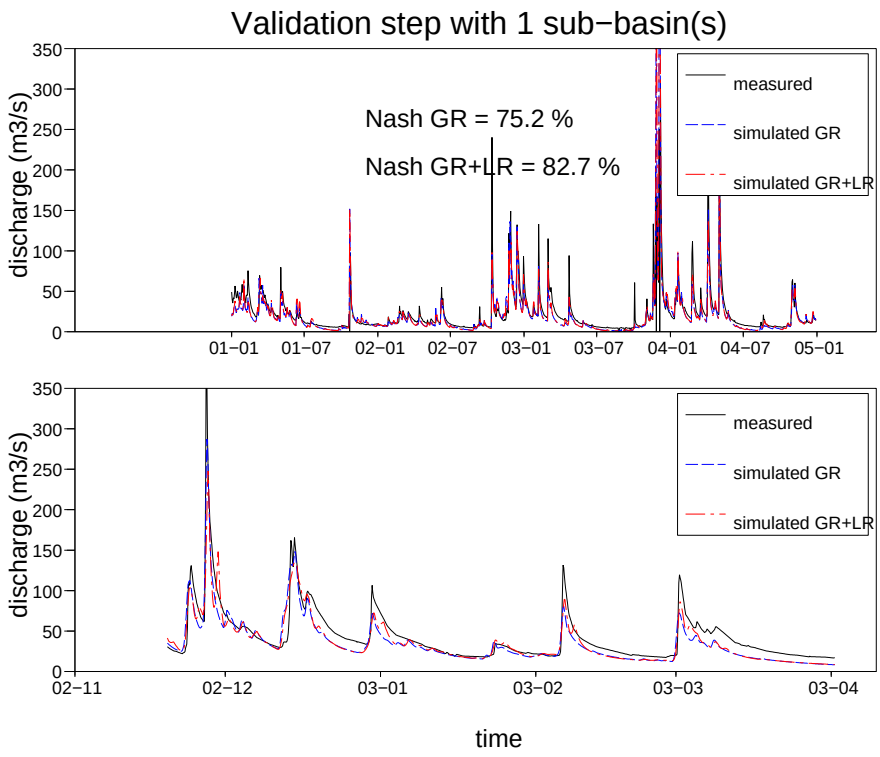

Figure 6: Validation step. Discharge at the downstream end of the channel (on the whole validation period and zoom): (− −) measurements, (···) GR simulation, (—) GR+LR simulation with one sub-basin.

high flows. For instance, a Nash-Sutcliffe coefficient calculated on the logarithm of the discharge gives the same weight to the relative error $(Q_s - Q_m)/Q_m$, whether in high flow or in low flow.

5 Conclusion

This paper proposed a new theoretical framework to take account of the lateral discharge in the flow routing process. The transfer functions are obtained in a closed form in the Laplace domain. A first-order approximate model leads to an ordinary differential equation in the time domain, which gives a quick computation method for the flow routing model.

The method allows to evaluate the response of a watershed with known upstream discharge, rainfall and potential evapotranspiration. The lateral discharge is modeled by a four-parameter lumped rainfall-runoff model. The flow routing model can be parameterized with four physical parameters: mean discharge, mean slope, river width and Manning roughness coefficient. Therefore, the coupled model requires the calibration of only four parameters.

An illustration of the model is presented on the upper Tarn River. The contribution due to rainfalls can be integrated by considering different sub-basins. The example also shows that it is not always useful to consider a large number of sub-basins to improve the model performance at the downstream end of the watershed, but that the knowledge of the upstream discharge brings a lot of information even if the corresponding basin area is small compared to the whole basin.

For dam release management, it is essential to correctly represent the flow routing process at low discharge too. In these conditions, backwater and feedback effects due to cross devices may have a significant effect on the flow dynamics. The same theoretical approach can be developed accordingly, using for example an approximate determination of the water surface profile (Munier et al., 2007). It may be necessary to have a good estimate of the water withdrawals also. These withdrawals can be integrated the same way as the rainfall contributions, either as punctual or as distributed withdrawals.

References

Beven K., 2006 A manifesto for the equifinality thesis. *Journal of Hydrology*; 320(1-2):18-36.

Chow V., 1988. *Open-channel Hydraulics*. McGraw-Hill Book Company, New York. . 680 p.

Dooge J, Napiórkowski J, Strupczewski W., 1987a. The linear downstream response of a generalized uniform channel. *Acta Geophysica Polonica*;XXXV(3):279-293.

Dooge J, Napiórkowski J, Strupczewski W., 1987b. Properties of the generalized downstream channel response. *Acta Geophysica Polonica*;XXXV(6):967-972.

Fan, P. and Li, J.C., 2006. Diffusive wave solutions for open channel flows with uniform and concentrated lateral inflow. *Adv. Water Resour.*;29:1000–1019.

Litrico X, Fromion V., 2004a. Frequency modeling of open channel flow. *J. Hydraul. Eng.*;130(8):806-815.

Litrico X, Fromion V., 2004b. Simplified modeling of irrigation canals for controller design. *J. Irr. and Drain. Eng.*;130(5):373-383.

Malaterre, PO., 1994. Modélisation analyse et commande optimale LQR d'un canal d'irrigation. Ph. D. thesis, LAAS - CNRS - ENGREF - Cemagref. In French.

Moramarco, T. and Fan, Y. and Bras, R.L., 1999. Analytical solution for channel routing with uniform lateral inflow. *J. Hydraul. Eng.*;125:707–712.

Moussa, R., 1996. Analytical Hayami solution for the diffusive wave flood routing problem with lateral inflow. *Hydrol. Processes*;10:1209–1227.

Munier, S. and Litrico, X. and Belaud, G., 2007. Linear approximation of flood routing method with backwater effects. *Proceedings of the 32th IAHR Congress in Venice.*

Perrin, C., C. Michel, and V. Andréassian, 2003. Improvement of a parsimonious model for streamflow simulation *J. Hydrol.*; 279(1-4): 275–289.

Rey, J., 1990. Contribution à la modélisation et la régulation des transferts d'eau sur des systèmes de type rivière/baches intermédiaires. M. Sc. thesis, Université Montpellier 2. In French.

Tsai, C.W., 2003. Applicability of Kinematic, Noninertia, and Quasi-Steady Dynamic Wave Models to Unsteady Flow Routing. *J. Hydraul. Eng.*; 129(8): 613–627.

Weinmann P, Laurenson E., 1979. Approximate flood routing methods: A review. *J. Hydraul. Div., ASCE*; 105: 1521-1536.